npj | heritage science

Article

https://doi.org/10.1038/s40494-025-02233-5

The acid attack (1990) on Rembrandt's *The Night Watch* (1642). Reassessing the painting's condition through a multimodal analytical approach

Check for updates

Laura Raven[1,9] ✉, Arthur Gestels[2,3,9], Annelies van Loon[1,4], Ermanno Avranovich Clerici[2], Esther van Duijn[1], Mitra Almasian[1,5], Frederik Vanmeert[1], Steven de Meyer[2,6], Victor Gonzalez[1,7], Koen Janssens[2] & Katrien Keune[1,8]

In 1990, Rembrandt's *The Night Watch* was attacked with concentrated sulphuric acid. This study reassesses the affected area and aims to identify and characterise any secondary degradation products, as well as any challenges for the conservation treatment. A comprehensive analytical approach, using macroscopic X-ray fluorescence (MA-XRF), macroscopic X-ray powder diffraction (MA-XRPD), optical coherence tomography (OCT), and light microscopy, scanning electron microscopy combined with energy-dispersive X-ray (SEM-EDX) analysis, micro attenuated total reflectance Fourier transform infrared (μ-ATR-FTIR) spectroscopy and synchrotron radiation micro X-ray powder diffraction (SR-μ-XRPD) of three paint cross-sections, permitted the confirmation of anglesite ($PbSO_4$) and extensive lead soap formation in the affected areas. Additionally, mock-ups were prepared and analysed to reconstruct the entire sequence of events of the acid attack. Current estimations predict that some of the damage to the paint layers will become discernible after varnish removal and that local consolidation of the fragile surface might be required.

On the morning of Friday 6 April 1990, Rembrandt's *The Night Watch* (1642) was attacked at the Rijksmuseum in Amsterdam for the third time in its lifetime[1,2]. The painting, a large dynamic group portrait of militiamen painted for the great hall of the arquebusiers' civic guard headquarters (*Kloveniersdoelen*) in Amsterdam (Fig. 1A), was sprayed with concentrated sulphuric acid by a perpetrator with a documented history of mental illness. The resulting flow pattern of trails and drops spanned an area measuring ~79 cm in height by 52 cm in width, covering the face, neck, and right arm of Jan van der Heede, the red musketeer positioned on the far left, as well as the face of sergeant Reijer Engelen, the figure behind his right arm and shoulder, and the shield in the space between them (Fig. 1B). Fortunately, greater damage was averted thanks to prior emergency response planning, foresight and prompt action by the guards and conservation staff. The museum staff and press concluded afterwards that the shock caused by the acid attack was greater than the effective damage done to the painting.

The painting, which was lined with wax-resin in 1975/76 and had previously been varnished with a thick poppyseed oil-containing dammar solution in 1975/76 and 1981 for added protection in the event of an attack[3], was thoroughly sprayed with demineralised water in order to dilute, neutralise and remove the acid[4]. The sources seem to imply that six cannisters of water were sprayed in a mist of water droplets, with each cannister containing 8–10 l of water, amounting to a total of max. 60 l of water. Two scientists from the former Central Research Laboratory for Objects of Art and Science, Amsterdam (currently RCE) assessed the situation by taking acid value (pH) readings of the affected area after the spraying. With the pH of the surface close to that of the demineralised water, it was confirmed evidence that no further spraying was necessary[5,6]. The painting was

[1]Rijksmuseum, Conservation & Science, Amsterdam, the Netherlands. [2]University of Antwerp, Department of Physics, AXIS Research Group, Antwerp, Belgium. [3]University of Antwerp, Faculty of Applied Engineering, Department Electromechanics InViLab Research Group, Antwerp, Belgium. [4]Mauritshuis, Collection and Science, The Hague, the Netherlands. [5]Department of Biomedical Engineering and Physics, Amsterdam UMC, Amsterdam, the Netherlands. [6]Royal Institute for Cultural Heritage (KIK-IRPA), Brussels, Belgium. [7]Université Paris-Saclay, ENS Paris-Saclay, CNRS, PPSM, Gif-sur-Yvette, France. [8]Van 't Hoff Institute for Molecular Sciences, University of Amsterdam, Amsterdam, the Netherlands. [9]These authors contributed equally: Laura Raven, Arthur Gestels.
✉e-mail: l.raven@rijksmuseum.nl

Fig. 1 | Rembrandt van Rijn. *The Night Watch Militia Company of District II under the Command of Captain Frans Banninck Cocq*, 1642. Oil on canvas, 410 × 485 cm. Rijksmuseum, Amsterdam. A The painting in its current condition (before restoration) **B** Detail of a black and white picture taken immediately after the acid attack in 1990.

subsequently dried with white paper tissue, taken off the wall and unframed. The conservators involved evaluated the damage and concluded that only the varnish had been affected[4]. The painting was then treated (a more detailed discussion of which is provided below) and reinstalled within a matter of weeks.

This act of vandalism was not an isolated incident, but rather part of a series of attacks on works of art that occurred primarily in art galleries across Europe during the second half of the 20th century. These attacks involved the use of mechanical force (e.g. the use of knives), corrosive or non-corrosive substances, or a combination of the aforementioned, leaving many (old master) paintings severely damaged. In addition to the earlier (mechanical) attacks on *The Night Watch* in 1911 and 1975, a significant number of paintings by Peter Paul Rubens, Albrecht Dürer, Nicolaes Maes and Willem Drost, as well as three other works by Rembrandt, were subjected to acid attacks in museums such as the Alte Pinakothek in Munich (1959 and 1988)[7–11], the Gemäldegalerie in Düsseldorf (1977)[12], the Gemäldegalerie Alte Meister in Kassel (1977)[13,14] and the State Hermitage Museum in St. Petersburg (1985)[15].

The emergency response in these museums was contingent upon the nature of the collection, and the condition and the (conservation) history of the affected paintings played a significant role in the nature of the damage. Some examples of the damage observed by the acid attacks included paint swelling, crust formation, the mixing and displacement of paint and varnish, and the deterioration of the support. It is noteworthy that, with the exception of the Rijksmuseum and the Hermitage[16], museums were notably reserved in their utilisation of water out of fear of promoting further damage. In one instance, the relative humidity was even kept significantly reduced to 35-37% for some time after the attack[10]. This sentiment concerning the potentially exacerbating nature of water is still shared today by institutions such as The National Gallery in London and The Courtauld Institute of Art after testing a range of corrosive substances on dummies and test paintings during in-depth studies and practical workshops[17–20]. Whilst water did not appear to have an adverse impact on the paint layers of *The Night Watch*, it is important to consider the role of the hydrophobic nature of the paint caused by the wax-resin lining and the thick varnish, and whether the water spraying method would have been as successful on any other painting in the Rijksmuseum galleries, especially those not wax-resin lined. Furthermore, the canvas impregnation, ground and paint layers are all oil-based, rendering them less water-sensitive than, for example, the ground layers observed in Dürer's paintings[7–11].

In 2019, *Operation Night Watch* was launched: the largest interdisciplinary research and conservation project of *The Night Watch* to date. This initiative presented a timely opportunity to reassess the affected area, given the significant advancements since 1990 in the development of analytical techniques, especially in the field of non-invasive imaging techniques[21–25]. At the time of the initial investigation in 1990, the scientists involved had already hypothesised that a small quantity of the sulphuric acid could have reacted with chalk and lead white inside the paint to form calcium sulphates (e.g. $CaSO_4.2H_2O$, gypsum or $CaSO_4$, anhydrite) and lead sulphates (e.g. $PbSO_4$, anglesite or $K_2Pb(SO_4)_2$, palmierite)[26,27], as has also been the case in other paintings affected by acid attacks[9,12,13]. However, as no visible damage to the paint layers was observed following the attack, no further analysis was conducted to monitor the formation of any secondary degradation products. Given the association of lead sulphates with issues such as consistency changes of the paint[9,13], which could potentially complicate the conservation treatment, verifying their potential formation was highly relevant.

The central question this paper addresses is if the concentrated sulphuric acid affected the paint layers of *The Night Watch*, and particularly whether it led to the formation of lead-sulphur degradation products, due to the presumed greater impact of the sulphur on the paint layers compared to water. This information is important to identify any potential challenges for the painting's conservation treatment. The condition of the paint layers in the affected area was assessed by identifying any secondary degradation products at both macroscopic and microscopic levels using a wide range of complementary analytical techniques. These included macroscopic X-ray fluorescence (MA-XRF) imaging to determine the elemental composition of the paint layers; and macroscopic X-ray powder diffraction (MA-XRPD) imaging in reflection mode to identify and spatially map crystalline degradation products, and optical coherence tomography (OCT) to examine the varnish layers.

The non-invasive macroscopic imaging was complemented with the analysis of three micro-samples taken from both affected and unaffected nearby areas. The embedded samples were examined by scanning electron microscopy combined with energy-dispersive X-ray (SEM-EDX) analysis, micro attenuated total reflectance Fourier transform infrared (μ-ATR-FTIR) spectroscopy and synchrotron radiation micro X-ray powder diffraction (SR-μ-XRPD) analysis to gain a deeper insight in the stratigraphy and potential degradation of the paint. Additionally, a selection of varnish removal tests was conducted to further characterise the current condition of the paint layers. Finally, a series of mock-ups was prepared and exposed to sulphuric acid and subsequent water rinsing in order to gain further insight into the formation of anglesite, with particular attention paid to the influence of (1) the ground, (2) the composition of the pictorial layer, (3) the presence or absence of a varnish and (4) the time of exposure to drops of concentrated sulphuric acid.

Methods

Macro X-ray fluorescence (MA-XRF) imaging

The chemical elements mapping of *The Night Watch* was conducted by the *Operation Night Watch* team of the Rijksmuseum using macroscopic X-ray fluorescence (MA-XRF) imaging spectroscopy. The painting was scanned over the course of three months and in order to scan it as a whole, the painting was divided into 56 different sections, each measuring 580 × 780 mm. The analyses were performed with a M6 Jetstream (Bruker Nano GmbH, Berlin, DE) MA-XRF scanner[22]. The scanner is equipped with a 30 W Rh-target microfocus X-ray tube with a maximum voltage of 50 kV, a maximum current of 0.6 mA, a polycapillary lens, and two 60 mm^2 X-Flash silicon drift detectors that are moved over the surface of the painting by means of an X,Y-motorised stage. The measurements were performed by collecting X-ray photons emitted by the painting material, employing a spot-size of the primary X-ray beam of around 250 μm, an acquisition time of 35 ms per point and a step size of 500 μm. In addition to the scanning of the entire painting, high-resolution detail scans were taken from specific areas, including the c. 90 × 110 mm detail of the acid attack (no. D00), with an acquisition time of 110 ms per point and a step size of 250 μm. Finally, the acquired data cubes were then exported and processed using the PyMca and Datamuncher software packages to produce the elemental distribution maps[28,29].

Macro X-ray powder diffraction (MA-XRPD) Imaging

The MA-XRPD measurements on *The Night Watch* were performed by means of an in-house built mobile scanner (AXIS, University of Antwerp, BE)[21]. The device is set-up with a low power X-ray micro source (50 W, IμS-Cu, Incoatec GmbH, DE) that produces a monochromatic and focused X-ray beam (Cu–K_α; 8.04 keV) with a photon flux of 2.9×10^8 photon s^{-1} (focal spot diameter: ca. 140 μm, output focal distance: ca. 20 cm and a beam divergence: 2.4 mrad). A primary beam impingement angle of 10° relative to the surface of the painting was chosen. This resulted in an elliptical beam footprint with dimensions of 0.8 mm in the horizontal and 0.2 mm in the vertical direction. To record 2D diffraction patterns at each measurement position, A PILATUS 200K (DECTRIS Ltd., CH) area detector was utilised. All components were mounted on a motorised platform capable of movement in the X, Y and Z directions. To mitigate the impact of local topography and curvature of the painting surface on the diffraction data, the distance between the artwork and the scanner was automatically adjusted using a laser distance sensor (Baumer GmbH, DE) at all positions. The in-house developed software package XRDUA was utilised for the processing of the diffraction data. XRDUA provides the necessary tools for extracting crystalline-specific distributions from the large number of 2D diffraction patterns obtained during XRPD imaging experiments[30].

Optical coherence tomography (OCT)

Optical Coherence Tomography (OCT) images were collected using two OCT devices. The Thorlabs Ganymede OCT device functioning at the centre wavelength of 930 nm. The axial and lateral resolution were 3.0 micrometre in air and 8.0 micrometre, respectively. Volumetric images were collected of an area of 7 by 3 mm using 1024 by 1024 pixels. The OCT Images were post-processed using ImageJ version 1.54 f, whereafter the varnish and paint layer were segmented in automated fashion and corrected for the refractive index using a custom developed script in MATLAB version 2020a [Natick, Massachusetts: The MathWorks Inc.] to obtain the height maps. A refractive index of 1.5 was used for varnish to convert optical pathlength to physical distance.

Paint micro-samples and sample preparation

Three samples were taken in the acid attack area in *The Night Watch*. Sample SK-C-5_024a was taken in a highlight of the right hand palm of Jan van der Heede, the musketeer in red. Additionally, two samples were taken in the grey shield grey shield behind him. Sample SK-C-5_035 was taken from within an acid trail and sample SK-C-5_036 was taken from a nearby unaffected area (see Supplementary Fig. 2).

The paint samples were prepared as cross-sections by embedding them in Technovit 2000 LC mounting resin - a one-component methacrylate that cures under visible blue light (Heraeus Kulzer GmbH, Germany) - (SK-C-5_024a) or Poly-pol PS230 polyester mounting resin with M.E.K.-peroxide harder (Poly-Service, Amsterdam, Netherlands) (SK-C-5_035 and SK-C-5_036) and polished using a sample holder and Micromesh sheets up to grade 12,000 (Micro-Surface Finishing Products Inc., Wilton, Iowa, USA) to expose the paint stratigraphy[31]. The cross-sections were examined using light microscopy, SEM-EDX, μ-ATR-FTIR, and SR-μ-XRPD.

Light microscopy

Light microscopy of the paint cross-sections was carried out on a Zeiss Axio Imager.A2m microscope equipped with a Zeiss AxioCam 506 colour digital camera. The cross-sections were examined in dark field (DF) mode and under ultraviolet radiation (UV365nm) at magnifications of up to 1000×. White light was provided by a LED lamp. For UV luminescence, a 365-nm LED Colibri 2 was used and a filter cube composed of a 365-nm excitation filter (EX G365), a beam splitter at 395 nm (BS FT 395), and an emission longpass filter at 420 nm (EM LP 420). Images were captured at spatial resolutions of 0.27 μm/pixel (200x) and 0.11 μm/pixel (500×) using the image-acquisition software Zen 2 pro (blue edition) with extended depth of focus (MEDF) facilities.

Scanning electron microscopy energy-dispersive X-ray (SEM-EDX) spectroscopy

Scanning electron microscopy in combination with energy dispersive X-ray spectroscopy (SEM-EDX) was performed on a FEI NovaNano SEM 450 variable pressure electron microscope equipped with a ThermoFisher NSS EDX system. The uncoated samples were first examined under low vacuum and backscattered-electron (BSE) images were collected at an acceleration voltage of 15 kV, spot 3, GAD detector, 90 Pa and a 5 mm eucentric working distance. The samples were then analysed under high vacuum with a thin gold coating (SK-C-5_024a) or a 4 nm thick tungsten coating using a Leica EM ACE600 Coater (8E−3 mbar) (SK-C-5_035 and SK-C-5_036) to improve surface conductivity. The EDX maps were also collected under high vacuum conditions, with an accelerating voltage of 20 kV, spot 5 and a map resolution of 1024 by 682 pixels, 60 s frame time, 85 μs dwell time and a total of 30 frames.

Micro attenuated total reflectance Fourier transform infrared (μ-ATR-FTIR) spectroscopy

FTIR spectral data of cross-sections SK-C-5_035 and SK-C-5_036 were collected employing the Perkin Elmer Spectrum 100 FTIR spectrometer combined with a Spectrum Spotlight 400 FTIR imaging system equipped with a 16 pixel mercury cadmium telluride linear array detector (16/2 MCT). A Perkin Elmer ATR imaging accessory consisting of a germanium crystal was used to impinge the sample prior to data collection. The spectral resolution employed corresponded to 16 cm^{-1} while the mapped area

shown in S.I. measured was 400 by 400 μm² in size employing a spatial resolution of 1.56 μm per pixel.

Synchrotron radiation micro X-ray powder diffraction (SR-μ-XRPD)

The SR-μ-XRPD analysis was performed at two different beamlines: P06 (PETRA III, DESY, DE) and ID13 (ESRF, FR). At ID13, the analysis was conducted on reconstructions only; at P06, however, all three cross-sectioned paint samples were examined in addition to the reconstructions. P06 is a hard X-ray micro- and nanoprobe beamline suited for XRPD imaging experiments on the microscale. A Kirkpatrick-Baez optical system was utilised to focus the beam to a diameter of 0.5 μm and a flux of 10^{10} photons s^{-1} with selected primary energies of 13 and 21 keV. The samples were positioned within a sample holder capable of movement in the X, Y and Z directions across several millimetres. An EigerX 4 M detector (DECTRIS Ltd., CH) was employed to collect the diffraction signals. The collected diffraction data were corrected for attenuation effects.

The ID13 beamline is an ESRF undulator beamline dedicated to high-lateral resolution diffraction and scattering experiments using focused monochromatic X-ray beams. The ID13 beamline offers high-brightness (sub)micrometric X-ray beams coupled with fast-reading, highly sensitive area detectors. This combination makes the beamline ideal for scanning experiments at high spatial resolutions. The mock-up samples were primarily investigated at the ESRF, where a rapid acquisition time enabled comprehensive analysis at the micro-branch end station. Samples were mounted vertically, perpendicular to the X-ray beam, and the energy of the incident beam was selected to be ~13.0 keV. The beam was focused to ≈2 × 2 μm² (flux ~2 × 10^{12} ph/s, at I = 128 mA electron beam current; attenuated to ~10^{11} ph/s by detuning the undulator) using a compound refractive lens (CRL) set-up mounted in a transfocator. SR-μ-XRPD maps were obtained by raster-scanning the samples and collecting 2D XRPD patterns, in transmission, similarly to P06. Additionally, this beamline employs an EigerX 4 M (DECTRIS Ltd., CH) single photon counting detector that acquires frames with 2070 × 2167 pixels (75 μm pixel size). Access to beamtime at ESRF was facilitated by the *Historical Materials BAG*[32].

Stereomicroscopy

The paint surface was examined using a Zeiss Stemi 508 stereomicroscope equipped with a Zeiss Axiocam 503 colour digital camera.

Varnish removal tests

The varnish removal test (test no. SK-C-5_005-0025E) discussed in this paper was conducted with 1 × 1 cm Evolon® CR (manufactured by Freudenberg, marketed by Deffner & Johann), a non-woven polyamide/polyester tissue[33,34]. The tissue was loaded with a 45% ethanol load a day prior to testing, and then brought into contact with the varnish surface and covered with Mylar®. After a 60-second contact time, the tissue containing the dissolved and absorbed varnish was removed.

Mock-up sample design and preparation

The objective was to create model samples that were as representative as possible of *The Night Watch* and the acid attack event. Eighteen of the thirty-six mock-ups were prepared with a preparation and ground layer (code **G**); the other half of the mock-ups only have a support and a pigmented layer (code N). A varnish layer was applied to half of the mock-up samples (code **V**; the unvarnished samples have code **U**). The stratigraphy of the mock-up samples was as follows:

0. *Support*: polycarbonate slide (the choice for a polycarbonate substrate in lieu of canvas was to allow for an easier preparation of the microtomed cross-sections).

1. *Preparation layer*: composed of a mixture of lead-rich linseed oil and sand (composed of pure quartz crystals: SiO_2), with an average thickness of less than 50 μm. Pure litharge β-PbO was amalgamated with oil in a ratio of 1:10 by weight, subjected to boiling (temperature between 180 and 200 °C) and reaction until all PbO particles were no longer discernible following a recipe by Turquet de Mayerne (1573–1654)[35]. The identification of a lead and oil-rich sizing layer was previously identified and discussed by Broers et al.[36]. The addition of sand to the leaded oil layer was to ensure its adhesion to the polycarbonate substrate.

2. *Ground layer*: composed of a quartz-rich clay mixed with linseed oil obtained with m% of 3:1 to obtain a workable paste to apply on top of the preparation layer[37].

3. *Pigmented layer*: All thirty-six samples were prepared employing paint with different lead white content in the pigmented layer but always keeping the same m% between pigments and oil of 1:3;

- with pure (hydrocerussite-rich) lead white; sample code: 100% (reflecting the mass percentage of lead white in oil);
- with a mixture of lead white (20 m%), ochre (20 m%), bone black (20 m %), vermillion (20 m%), and madder lake (20 m%); sample code: 20%;
- with a mixture of lead white (10 m%), ochre (22.5 m%), bone black (22.5 m%), vermillion (22.5 m%), and madder lake (22.5 m%); sample code: 10%.

4.*Varnish layer*: A newly prepared varnish, characterised by the same composition as the varnish applied in 1975 by Kuiper (30 parts turpentine oil, 10 parts dammar and 1 part poppyseed oil by volume) was employed to varnish the mock-ups[3].

Following the preparation, the simulation samples were then subjected to artificial ageing for a period of 450 h (~19 days) in a climate chamber (UV 200RB/20 Weiss Technik, BE). The purpose of this process was to weaken and degrade the protective varnish (if present) and the oil binder. To achieve this, lamps were utilised that imitated sunlight, operating at a fixed temperature of 50 °C and a relative humidity of ~80%.

The mock-up samples were sprinkled with a concentrated sulphuric acid solution (≥95 w%) to replicate the acid attack in 1990 and to ascertain the effect of different contact times between the acid and the pictorial stratigraphy. To emulate the swift intervention of museum security personnel, three different contact times were employed: 5, 10 and 20 min, respectively (with designated sample codes 5 min, 10 min and 20 min). After the termination of a designated timeframe, the paint surface, held vertically, underwent extensive rinsing with deionised water for a duration of 15–20 min to remove the sulphuric acid solution, thus simulating the intervention of the museum staff after the attack. While the precise duration of the spraying has not been documented, it is generally assumed, based on circumstantial evidence and oral sources, that it took a significant amount of time.

Following the exposure to the acid and the water spraying, the thirty-six mock-up samples were subjected to a second round of artificial ageing for 448 h. This was conducted under similar conditions as the previous round (50 °C and 80% relative humidity) with the same lamps previously described. These conditions were selected to promote ion- and compound migration within and among the paint layers of the mock-up samples.

Results

The current condition of the paint and varnish layers

On initial observation, *The Night Watch* does not bear witness to the acid attack of 1990. Under regular light circumstances its condition remains seemingly unaffected after all these years. Even at close range, no clear acid flow pattern can be distinguished and subtle changes caused by the attack are easy to miss. However, in raking light, it becomes evident that the varnish applied over the affected area is slightly more matt and possibly also thinner than in the surrounding areas. This is corroborated by observations in UV-induced fluorescence, in which the flow pattern can easily be recognised, and where the varnish shows a weaker fluorescence in the areas that have been in contact with the sulphuric acid (Fig. 2). This difference in fluorescence is probably the result of the varnish being thinner, younger and of a slightly different composition[4]. OCT measurements confirmed that the varnish is indeed much thinner in the trails (see Supplementary Fig. 1).

Despite assurances of the former conservation staff that solely the varnish had been affected, and that the paint layers had remained unscathed, the precise extent of the impact on the varnish remains uncertain, with the possibility that it might have been lost entirely in some areas and that some of the sulphuric acid did in fact reach the paint. There is no known written report of the precise condition and nature of the conservation work carried out at the time. Oral accounts suggest that, where possible, the degraded and embrittled varnish was mechanically removed using small brushes before new dammar varnish was applied, first locally, then with a final overall layer[4,38]. It is unclear whether solvents were employed in the removal process, and to which extent residual varnish was left on the paint surface. Given the time constraints under which the remedial treatments were conducted, it is plausible that varnish residues swollen by the acid may have remained on the paint surface.

Fig. 2 | Detail of the current situation of the acid attack area of *The Night Watch* in UV illumination showing the musketeer in red, Jan van der Heede.

Close examination of the paint surface under high magnification (up to 50×) reveals that the paint layers did, in fact, suffer the consequences of the attack, particularly in the lead white-rich areas. In some areas, most notably in the white cuff of the red musketeer, crystalline-looking surface deposits are visible on the flattened tops of thick lead white brushstrokes (Fig. 3A). It appears that some type of reaction has taken place with the lead white, and that the flattening is either due to corrosion of the paint by the acid or the softened paint being abraded during the subsequent varnish treatment. This phenomenon is also visible in other areas of the acid attack area where lead white is present in the upper layers of the paint stratigraphy, but not in areas outside the acid trails.

After varnish removal tests, it was possible to obtain an unobstructed view of the paint layers in a few selected locations within the acid attack area (Fig. 3B–D). In the grey shield, the trails marked by the acid become clearly visible without the presence of a varnish (Fig. 3B, C). High-magnification examinations of the paint surface confirm the flattening and abrasion of the tops of brushstrokes. Here it appears as if the acid has caused the top layer to react away, exposing the lead white-containing underlayer. Pigment particles lay bare, and the paint surface appears to be highly porous and broken up, manifesting as a pitted appearance. A comparable porosity was observed in the Munich Dürer paintings, and it was partially attributed to the formation of CO_2 gas bubbles shortly after the attack[9]. It is plausible that some of the round craters in *The Night Watch* paint surface are caused by the same type of process, albeit on such a superficial level and small scale that the bubbling effect of the acid may not have been observed at the time.

The desaturated, whitened appearance of the paint surface of the grey shield visible after varnish removal is most probably caused by a scattering effect of the porous, roughened surface. As this issue mostly disappears after temporarily saturating the surface with ShellSol T (aromatic-free hydrocarbon solvent), it is hypothesised that the binder may have been affected by

Fig. 3 | Stereoscopic micrographs of the paint surface revealing traces of the acid attack. **A** Flattened brushstrokes and crystallisation are visible in the white cuff (indicated with arrows). **B** The same type of flattening is visible in raking light in an acid trail (indicated with white dashed lines) in the grey shield after varnish removal. **C** Upon closer inspection it becomes apparent that the grey surface layer is absent, and that the white layer beneath is very porous. **D** Upon temporary saturation with ShellSol T some of the paint degradation becomes less visible due to reduced scattering of the broken-up surface.

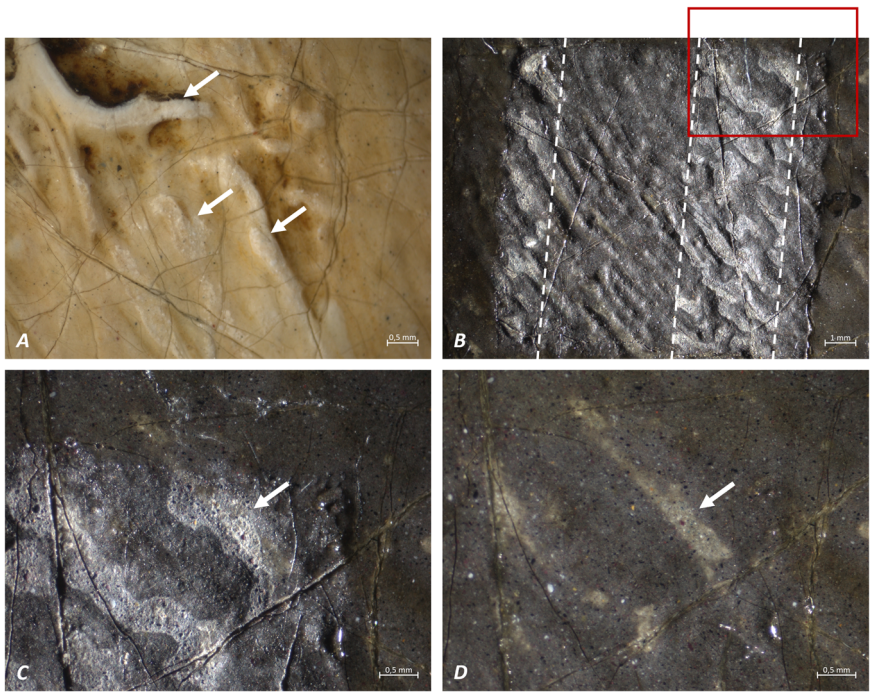

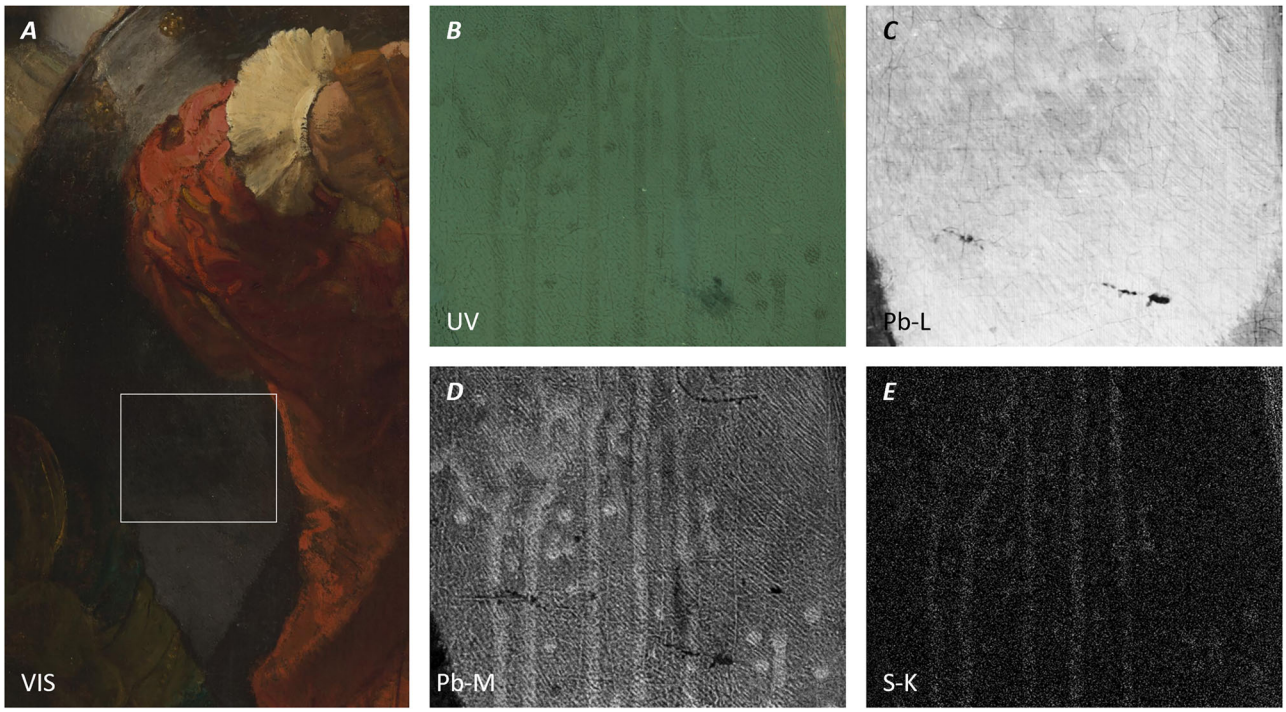

Fig. 4 | High-resolution MA-XRF imaging of the acid attack area in *The Night Watch*. **A** Detail of the grey shield in VIS and **B** in UV light; MA-XRF distribution maps (scan location marked in white in (**A**)) of: **C** Pb-L, **D** Pb-M and **E** S-K. Brighter areas indicate a higher elemental intensity.

the acid to some degree (Fig. 3D), as was also the case in Rembrandt's *Danaë*[39]. In this context, "saturating" refers to the (temporary) visual deepening and clarification of the paint layer when a varnish (or in this case a solvent) reduces surface scattering by wetting and thus unifying the surface, allowing the original colour and tone to appear more vivid. It is expected that, similarly to the application of ShellSol T, a newly applied varnish will most likely also visually negate this effect. However, as the painting is set to undergo a comprehensive restoration treatment, including the complete removal of the existing varnish, it is essential to gain a thorough understanding of the chemical degradation of the paint within the acid attack area, and how it could potentially affect the treatment.

MA-XRF imaging

In the grey shield (Fig. 4A), the acid flow pattern can be clearly identified in the high-resolution elemental distribution maps of lead (Pb-M, Fig. 4D) and sulphur (S-K, Fig. 4E), and corresponds precisely to the pattern captured in a photograph from 1990 (Fig. 1B) and in UV (Fig. 4B). The absence of this pattern in the L-line mapping of lead (Fig. 4C) suggests that the attack predominantly modified the chemical composition of the surface layers of the paint stratigraphy. Pb-L signals are of a higher energy and convey information from both surface and deeper layers within the paint stratigraphy (<200 µm) in comparison to the lower energy Pb-M photons, which mainly arise from areas located closer to the surface (<10 µm). The sulphur S-K photons are in the same energy range as the Pb-M photons and must also derive from the upper layer(s).

Elevated Pb-M and S-K intensities were discerned in the acid trails when compared to the surrounding paint. The direct contact between lead ions and sulphuric acid may have resulted in the potential precipitation of one or more insoluble lead-sulphur compounds on the surface. It is hypothesised that the sulphur detected in this area derives from the presence of a newly formed secondary compound, as can be observed in the diffraction and SEM-EDX images (see Figs. 6 and 7), rather than from free sulphuric acid left in the paint or varnish. However, further characterisation is necessary to ascertain the precise origin of the sulphur in question. This includes determining whether the formation of sulphur-rich products is confined to the uppermost 10 µm of the paint stratigraphy, or if they have also formed deeper within the paint. Care should be taken when interpreting the Pb-M map. As OCT confirmed that the varnish in the acid trails is thinner than in the adjacent regions, it will cause less attenuation of the Pb-M signal emerging from underneath. Additionally, the potential migration of lead ions into the superficial regions of the varnish may be a contributing factor as well. Finally, the partial spectral overlap between the Pb-M and S-K lines must be considered, as this can artificially enhance the apparent Pb distribution in areas where anglesite is present.

MA-XRPD imaging

Figure 5E–G present the macroscopic distribution maps of the most relevant identified crystalline phases (measured down to a depth of 10 µm) within a small area of the affected region. This area encompasses part of a metal shield and part of the right leg of sergeant Reijer Engelen (Fig. 5J), the figure seated on the right side of Jan van der Heede, the musketeer in red (Fig. 5A). In the leg of the former, calcite ($CaCO_3$) was discovered alongside weddellite ($CaC_2O_4{\cdot}2H_2O$) (Fig. 5E), a calcium-containing alteration product that is frequently encountered in paintings[21,40,41].

In the area examined, lead white was predominantly identified in the light grey highlight of the grey metal shield, as illustrated in Fig. 5I. This highlight is characterised by an abundance of hydrocerussite ($2PbCO_3{\cdot}Pb(OH)_2$), along with a minor presence of cerussite ($PbCO_3$). Additionally, two lead-sulphur-containing alteration products, palmierite ($K_2Pb(SO_4)_2$) and anglesite ($PbSO_4$), were also identified. Their distribution is shown in Fig. 5F and G, respectively.

The distribution of palmierite (Fig. 5G) is akin to that of potassium (Fig. 5D), which is present in the leg of sergeant Engelen. It is widely acknowledged that palmierite frequently develops in areas where potassium-containing pigments, such as smalt, organic lakes, ultramarine, and earth pigments, are present alongside lead-containing pigments such as lead white[21,27,42,43–49]. The Pb-M map (Fig. 5C) indicates that lead is indeed present in this area, albeit to a lesser extent than in the shield. Interestingly, the distribution map of palmierite (Fig. 5G) does not appear to exhibit the distinctive drip pattern (Fig. 5C), contrary to that of anglesite (illustrated in Fig. 5F). The latter compound is less frequently encountered in oil paintings and was also not identified in other areas of *The Night Watch* that were

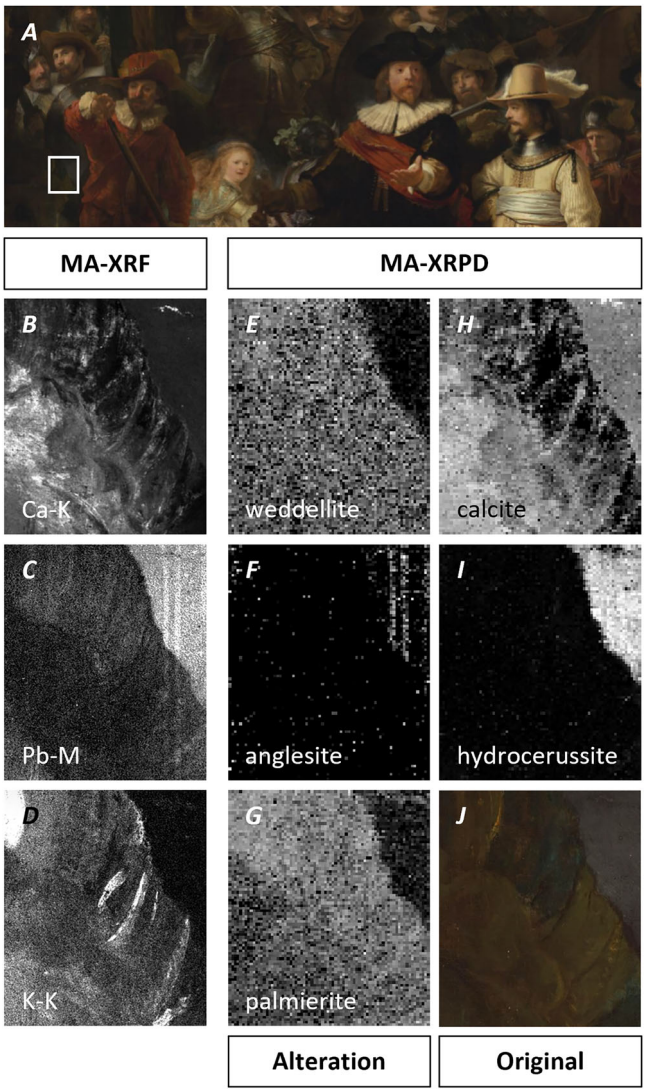

Fig. 5 | MA-XRF and MA-XRPD imaging of the acid attack area in *The Night Watch*. **A** The area investigated is marked in white; MA-XRF distribution maps of: **B** calcium (Ca-K), **C** lead (Pb-M) and **D** potassium (K-K); Corresponding MA-XRPD distribution maps of: **E** weddellite, **F** anglesite, **G** palmierite, **H** calcite and **I** hydrocerussite; **J** subarea within the acid attack area. Brighter areas indicate a higher XRF or XRPD intensity value.

analysed using MA-XRPD[50]. As illustrated in Fig. 5G, palmierite has formed in the leg of the seated musketeer, creating a fairly uniform sulphate-rich layer. It seems plausible to suggest that this layer has probably formed gradually over the 400-year existence of *The Night Watch*, which would have resulted in the majority of the K^+ ions being trapped within the palmierite precipitate. Following the acid attack, the absence of an adequate concentration of available K^+ ions within the affected area may have hindered the local precipitation of additional palmierite (Fig. 5D), allowing solely the formation of anglesite as a secondary product.

Paint cross-sections

Three cross-sectioned samples from the acid attack area in *The Night Watch* were subjected to comprehensive analysis in order to ascertain whether the formation of anglesite was indeed caused by exogenous factors such as the sulphuric acid attack, and not by natural alteration (i.e. pigment and binder interaction over the course of time). Two of the samples were taken in close proximity to each other in the grey shield: one sample inside one of the acid trails (SK-C-5_035) and the other in an unaffected area just outside of a trail (SK-C-5_036) (Fig. 6, and Supplementary Fig. 2). The third sample was obtained from the end of an acid drip in a lead-rich highlight on the proper right palm of the red musketeer (SK-C-5_024a) (Fig. 7, and Supplementary Fig. 2). Their location was selected based on the results obtained through MA-XRF and MA-XRPD and the confirmed presence of lead white and anglesite.

During sampling of cross-section SK-C-5_024a, it was observed that the paint exhibited a notable degree of softness and a consistency reminiscent of butter, which is contrary to the characteristics one would typically associate with a lead-rich 17th-century oil paint. This type of softening of lead white-containing paints has been observed in other paintings following acid attacks and has been attributed to the conversion of lead carbonate to lead sulphate[9,13]. The concentrated sulphuric acid may also have affected the oil binding medium, such as causing hydrolysis of the ester bonds, which can also lead to softening of the oil paint. Given that no softening was observed during sampling in the shield, it was hypothesised that the higher lead white content and longer exposure to a greater quantity of sulphuric acid at the end of the acid trail were responsible for the change in consistency and hardness of the paint in the hand. A similar observation or even a more marked reaction at the end of acid drippings was also made after the attack of a painting by Rubens in Düsseldorf in 1977[12].

Figure 6 shows the light microscopy images of samples SK-C-5_035 and SK-C-036 in dark field (DF) and UV (365 nm) illumination, as well as the SEM-BSE images and a selection of SR-μ-XRPD maps (see also Supplementary Figs. 4, 5). The two samples contain the complete stratigraphy with the exception of the quartz-containing ground layer. The comprehensive microscale analysis reveals multiple brown and grey paint layers of similar composition; four in sample SK-C-5_035 and three in SK-C-5_036. Among a wide array of other pigments, lead white is present in varying quantities and condition states throughout the complete stratigraphy of both samples. Figure 7 illustrates the findings of the microscopic analysis of sample SK-C-5_024a, obtained from the hand palm of the red musketeer (see also Supplementary Fig. 3). As a result of the aforementioned difficulty encountered during the sampling process caused by the soft consistency of the paint, the sample comprises solely the uppermost paint layer, which is rich in lead white as well.

In the BSE images of the samples taken from the affected areas, SK-C-5_035 (Fig. 6C, D) and SK-C-5_024a (Fig. 7C, D), the dissolution of lead white pigment due to saponification (as substantiated by μ-ATR-FTIR analysis of sample SK-C-5_035, see Supplementary Fig. 6) becomes discernible in the BSE images as greyish areas or halos encircling the lead white particles. This phenomenon can also be recognised in sample SK-C-5_036 (Fig. 6I, J, Supplementary Fig. 7), albeit to a much lesser degree. Additionally, it becomes evident from the BSE images that the paint surface in the samples from the affected areas has been severely disrupted, characterised by an uneven and fragmented surface layer. The lead white exhibits an amorphous and light grey appearance, while the lead white particles in the surface layer of sample SK-C-5_036, taken from the unaffected paint, remain intact. In accordance with the findings of the surface examination, it can be hypothesised that (part of) the binding medium in the upper layer has reacted away (shown by layer 5a in Fig. 6D). In contrast, the BSE image of sample SK-C-5_036 does not demonstrate the aforementioned fragmented or irregular surface morphology, nor does it exhibit an absence of binding material (Fig. 6J).

Moreover, the SEM-EDX maps of sample SK-C-5_035 indicate an enrichment of sulphur at the paint surface (see Supplementary Fig. 4). A comparable phenomenon can be discerned for SK-C-5_024a, although the evidence is less conclusive (see Supplementary Fig. 3). As expected, this enrichment is not evident in sample SK-C-5_036 (see Supplementary Fig. 5). By means of SR-μ-XRPD, it is possible to identify and visualise the presence of anglesite in the top layer of the pictorial stratigraphy in sample SK-C-5_035 (Fig. 6F). The thickness of the anglesite layer in SK-C-5_035 is ~5–10 μm, which is consistent with the sampling depth of the MA-XRPD instrument employed during the macroscopic investigation. Interestingly, anglesite was confirmed to be present throughout the entire top paint layer (~30–40 μm) of sample SK-C-5_024a (Fig. 7G), rather than solely at surface level. It seems plausible to suggest that the deeper formation of anglesite can be partially attributed to the sampling location of sample SK-C-5_024a at

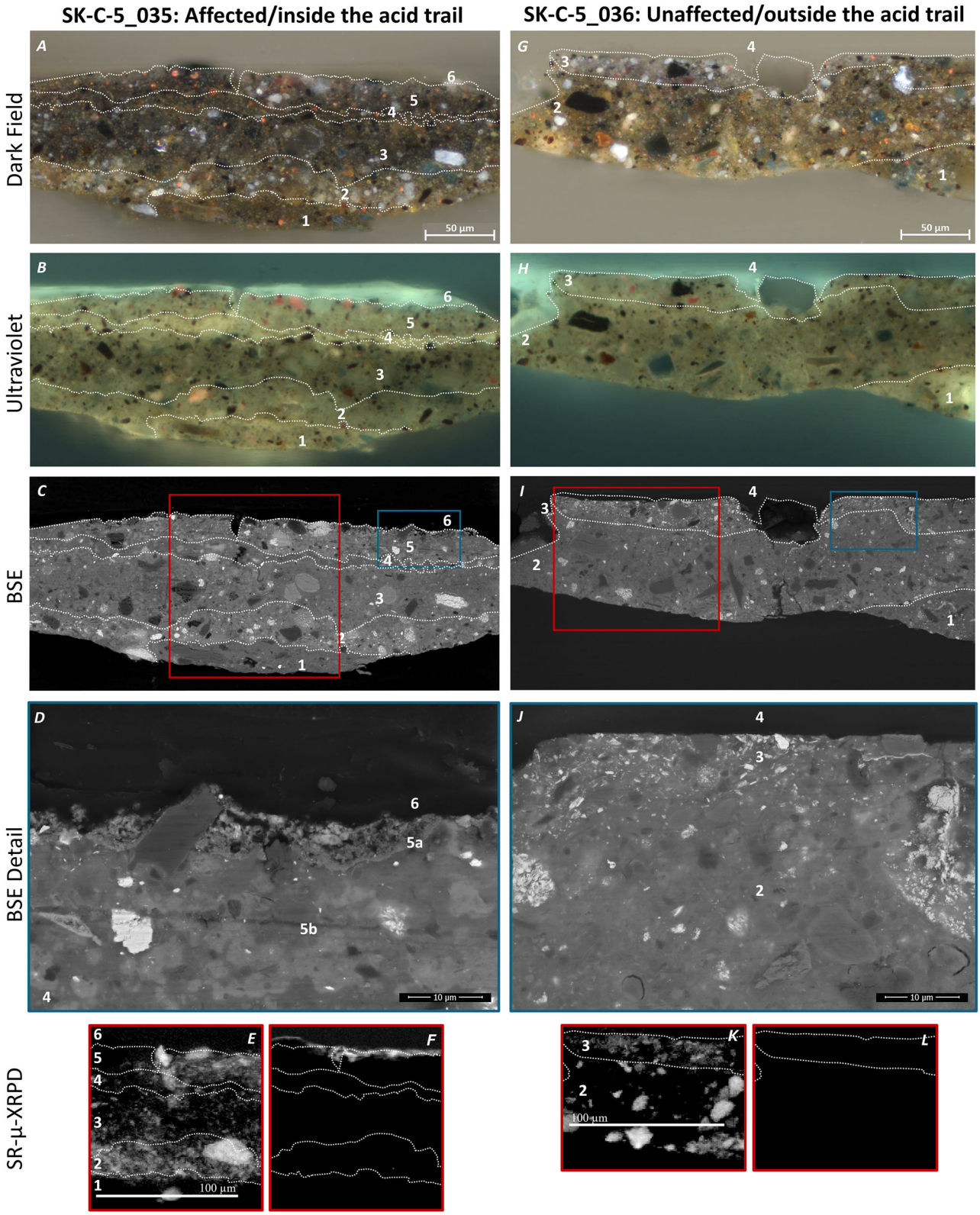

Fig. 6 | Results of the microscale analysis of cross-sections SK-C-5_035 and SK-C-5_036. Light microscopic images in dark field illumination (**A**, **G**) and UV light (**B**, **H**); Backscattered-electron (BSE) images (**C**, **I**); High-resolution BSE images (**D**, **J**) (location marked in blue in images **C**, **I**); SR-µ-XRPD maps (location marked in red in images **C**, **I**) showing the hydrocerussite (**E**, **K**) and anglesite (**F**, **L**) distributions. Brighter areas indicate a higher local abundance. Layer 1 in both paint samples contains a mixture of earth pigments, bone or ivory black, lead white, blue copper-containing particles (probably azurite), red lake, vermilion, some chalk and possibly smalt. Layer 2 in both samples contains the same pigments as layer 1. Additionally, these layers contain an organic brown (potentially Kassel earth), a few particles of gypsum and chalk and some lead-tin yellow. Layers 3 and 5 in sample SK-C-5_035 are similar in composition to layer 2, although they contain a higher amount of bone or ivory black. Layer 4 in this sample indicates interfacial material such as an oil skin, characterised by a high concentration of organic compounds. Layer 3 in sample SK-C-5_036 contains a mixture of bone or ivory black, (intact) lead white, vermilion, red lake, earth pigments and chalk. The top layer in both samples (layer 6 in SK-C-5_035, layer 4 in SK-C-5_036) is a natural resin varnish.

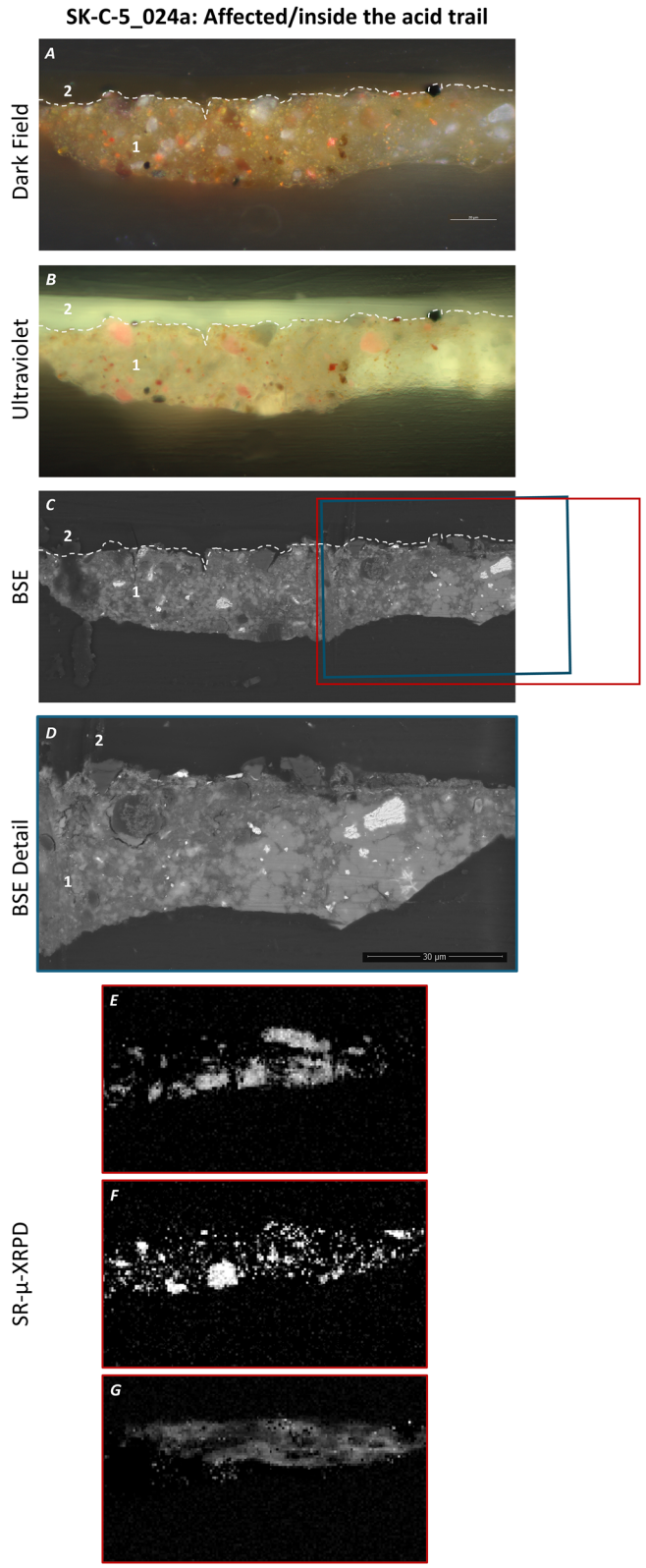

Fig. 7 | Results of the microscale analysis of cross-section SK-C-5_024a. Light microscopic images in dark field illumination (**A**) and UV light (**B**); Backscattered-electron (BSE) image (**C**); High-resolution BSE detail (**D**, **J**) (location marked in blue in image **C**); SR-µ-XRPD maps (location marked in red in image **C**) showing the hydrocerussite (**E**), cerussite (**F**) and anglesite (**G**) distributions. Brighter areas indicate a higher local abundance. Layer 1 contains vermilion, red lake, lead white, yellow earth, chalk and possibly smalt. Layer 2 is a natural resin varnish.

the end of the acid trail, which was exposed for a longer period of time and to a greater quantity of sulphuric acid in comparison to that of sample SK-C-5_035, which was taken in the middle of the trail. In comparison, in sample SK-C-5_036, which was sampled from a nearby area not affected by the sulphuric acid, neither anglesite nor any other crystalline sulphate could be detected.

Mock-up samples

To improve our comprehension of the interaction between the sulphuric acid and the paint layers, a series of 36 mock-up samples was prepared. The series comprised a number of variables, including (1) the presence or absence of the lead-rich preparation and ground layers. These were created by adding lead monoxide (PbO) to linseed oil as a drying agent. Furthermore, (2) the composition of the paint layer, (3) the presence or absence of varnish, and, (4) the time of exposure to drops of concentrated sulphuric acid were systematically varied. The latter was controlled by rinsing the mock-up with demineralised water after a set amount of time, simulating the emergency response protocol in the case of a corrosive attack. As illustrated in the overview of the mock-up samples in Table 1, each mock-up sample was assigned a unique code to describe the nature of each layer. These codes are used in the discussion below. A more detailed description of the mock-up sample preparation can be found in the methods section.

Initially, all mock-up samples were analysed with the MA-XRPD instrument to ascertain the formation of anglesite. The resulting data are presented in Table 1. Afterwards, all samples were analysed employing SR-µ-XRPD imaging analyses at the PETRA-III and ESRF synchrotron facilities to investigate the newly formed secondary compounds and their distribution.

A number of observations can be readily made:

1. It was observed that an increase in the exposure time of the paint to sulphuric acid from 5 up until 20 min resulted in a significant increase in the likelihood of anglesite formation.
2. The samples containing a greater quantity of lead white exhibited the formation of anglesite after a mere 5 min of contact time. Upon increasing the exposure time to 10 min, anglesite began to form with greater frequency. After 20 min of exposure time, anglesite was identified in nearly all mock-up samples.
3. During the scanning of the mock-up samples, the presence of palmierite was not confirmed, despite the use of a potassium-containing pigment, madder lake, in addition to lead white. This observation is at odds with historical samples, in which this secondary product was detected. This discrepancy is likely due to the substantial age difference between the historical and mock-up samples, as palmierite appears to form only over longer timescales under these conditions.

The SR-µ-XRPD analysis enabled the mapping of the distribution of anglesite in the cross-sections obtained from the mock-up samples (see Supplementary Fig. 8), and revealed that the thickness of the anglesite layer increases in proportion to the duration of the acid exposure. Subsequently, the impact of the paint layer's lead white concentration was examined. An increase in the quantity of lead white present in the paint layer will result in a greater availability of dissolved lead ions for the formation of anglesite. It may therefore be anticipated that a positive correlation will be observed between the abundances of lead white and anglesite. As illustrated in Table 1, a paint layer comprising 100% lead white typically leads to the formation of anglesite. The observed trend in the model samples is consistent with the expected outcome, namely that the amount of anglesite formed increases with the concentration of lead-containing pigment (in this case, primarily hydrocerussite). Three examples of anglesite distribution maps can be found in the supplementary information (see Supplementary Fig. 8). It is also noteworthy that even a low concentration of lead white (10%) can result in the formation of anglesite. However, this does not yield a complete layer of anglesite, but instead results in the formation of isolated spots of this precipitate. When the concentration of lead white in the pictorial layer is

Table 1 | Schematic overview of the 36 mock-up samples

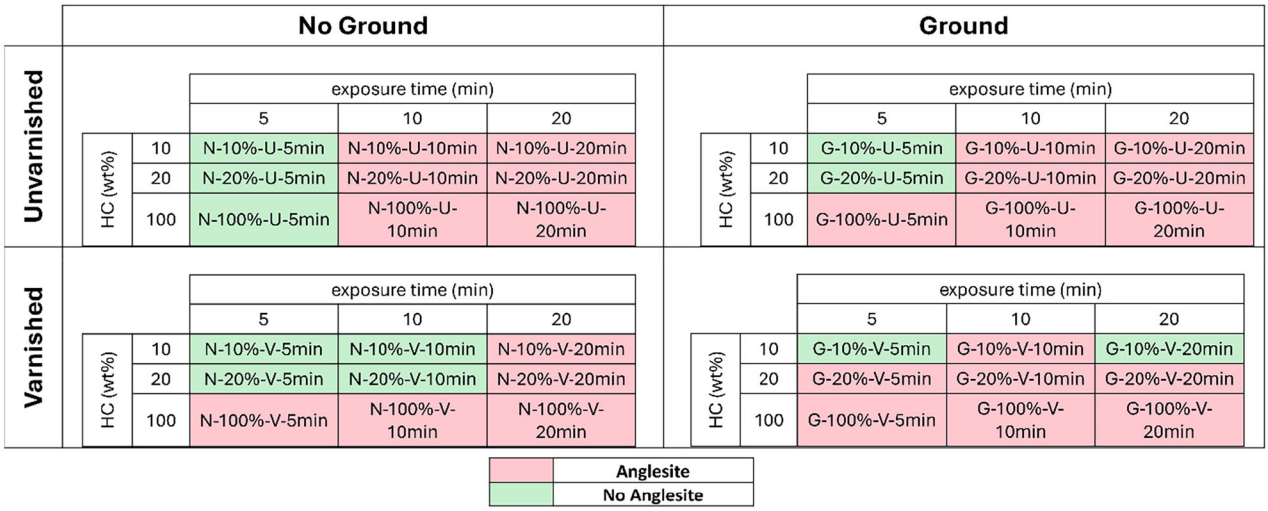

The following coding was used: G: PbO containing ground layer; N: no ground layer. 100%, 20% or 10%: marks the relative abundance of lead white used in the mock-up samples; other used pigments are ochre, bone black, vermillion and madder lake. V: varnished mock-up sample; U: unvarnished mock-up sample. 5 min, 10 min or 20 min marks the exposure time of the mock-up sample to sulphuric acid. Green cells indicate that anglesite was not identified; red cells indicate that anglesite could be identified by MA-XRPD.

increased to 20%, layered structures begin to form and become visible in the upper part of the paint layer.

Contrary to expectations, the anglesite distribution maps of varnish-covered mock-up samples (Fig. 8F, H) suggest that the presence of a varnish layer allows anglesite to form deeper below the surface compared to unvarnished mock-ups samples (Fig. 8B, D). Considering its significant oxidative power, it is not implausible that the sulphuric acid rapidly penetrates and partially dissolves ('eats away') the varnish layer. In such a situation, even after rinsing the paint surface with water, some (diluted) sulphuric acid might remain trapped in the remaining varnish, continuing to react with all materials in its proximity. In such a scenario, after water rinsing, the next critical step should then be to completely remove the varnish in affected areas to prevent residual acid from triggering further reactions; time would then be of the utmost importance, requiring swift intervention by the conservator. It should be noted however that the hypothesis that the varnish prevents some of the sulphuric acid from being rinsed away, needs to be investigated more in detail via a set of mock-up samples specifically designed for this purpose, which is beyond the scope of the current investigation.

The influence of the presence or absence of a ground layer containing PbO-rich oil has proven to be more complex to interpret. Table 1 indicates that when a lead-rich ground is present, anglesite is identified with greater frequency. This suggests that the PbO dryer may have acted as source of lead required for the formation of anglesite. However, when the distribution maps of anglesite of samples without and with a PbO-rich ground layer are compared (see Supplementary Fig. 8), only subtle differences are noticeable among both groups of mock-ups, rendering it difficult to draw any clear conclusion regarding the influence of the ground.

Discussion

Close examination of the paint surface and analytical research has revealed a discrepancy between the conclusions drawn shortly after the attack took place and the present findings. The initial conclusion that the paint had remained undisturbed can now no longer be maintained. The presence of crystalline surface deposits and a very broken-up and porous paint surface alluded to the disruption of both pigments and binding medium, which was confirmed by the identification of the lead sulphate anglesite. This principal secondary product resulting from the interaction of the sulphuric acid with the upper paint layer(s) of *The Night Watch* was found to form a crystalline precipitate at the paint surface composed of sulphate ions originating from the strong acid, and lead ions originating from lead white containing-paint.

The superficial distribution of anglesite is consistent with the photographs of the acid flow pattern taken immediately after the acid attack. Multimodal microscopic analysis of paint samples taken from within and immediately adjacent to the affected area confirmed the presence of anglesite in paint layers directly exposed to the sulphuric acid, down to a depth of ~5–10 µm in the middle of acid trails and 30–40 µm in areas that were exposed the longest. This resulted in the paint becoming porous and fragmented, or even soft at the bottom of the trail. Anglesite was not detected in the examined paint samples from *The Night Watch* at greater depths below the surface. This finding indicates that, while the impact of the sulphuric acid was not restricted to the varnish layers, it only affected the paint surface at a relatively superficial level. In contrast, no anglesite was encountered in areas not directly exposed to the acid.

The analysis of the series of paint mock-ups exposed to concentrated sulphuric acid and water rinsing indicates that it is possible to readily induce the formation of anglesite, resulting in a thin (ca. 10 µm) crust of crystalline lead sulphate that is very similar to that encountered in the affected areas of *The Night Watch*. Anglesite is formed in many circumstances even when only 10% of lead white is present. In the absence of a varnish layer, a mere 10 min of exposure time to sulphuric acid is sufficient to induce anglesite formation, irrespective of the other parameters investigated. The findings further demonstrate that, in the presence of a varnish, in situ formation of anglesite can be observed after 10 min when there is a lead-containing ground layer present and/or when the paint layer in contact with the acid is rich in lead white. Additionally, it has been demonstrated that any residual affected varnish may act as a trap for acid, thus potentially promoting any further reactions and damage. Consequently, complete removal of the varnish in similar scenarios is imperative.

Current estimations predict that some of the damage will become discernible after varnish removal and that the flow pattern of the attack will become identifiable as such. As evidenced by the varnish removal tests, the porous paint surface has been shown to cause a degree of light scattering due to binder-breakdown, which in turn has been demonstrated to result in a desaturating effect on the paint surface. Temporary saturation resolves this issue, and it is anticipated that a new varnish will produce a similar outcome. Further assessment of the paint surface after varnish removal will be necessary to ascertain whether local consolidation of the fragile surface will be required, especially where anglesite has formed. Adhering to varnish removal methods with low mechanical action will, it is predicted, avoid problems with the porous and potentially softened paint. Thanks to the

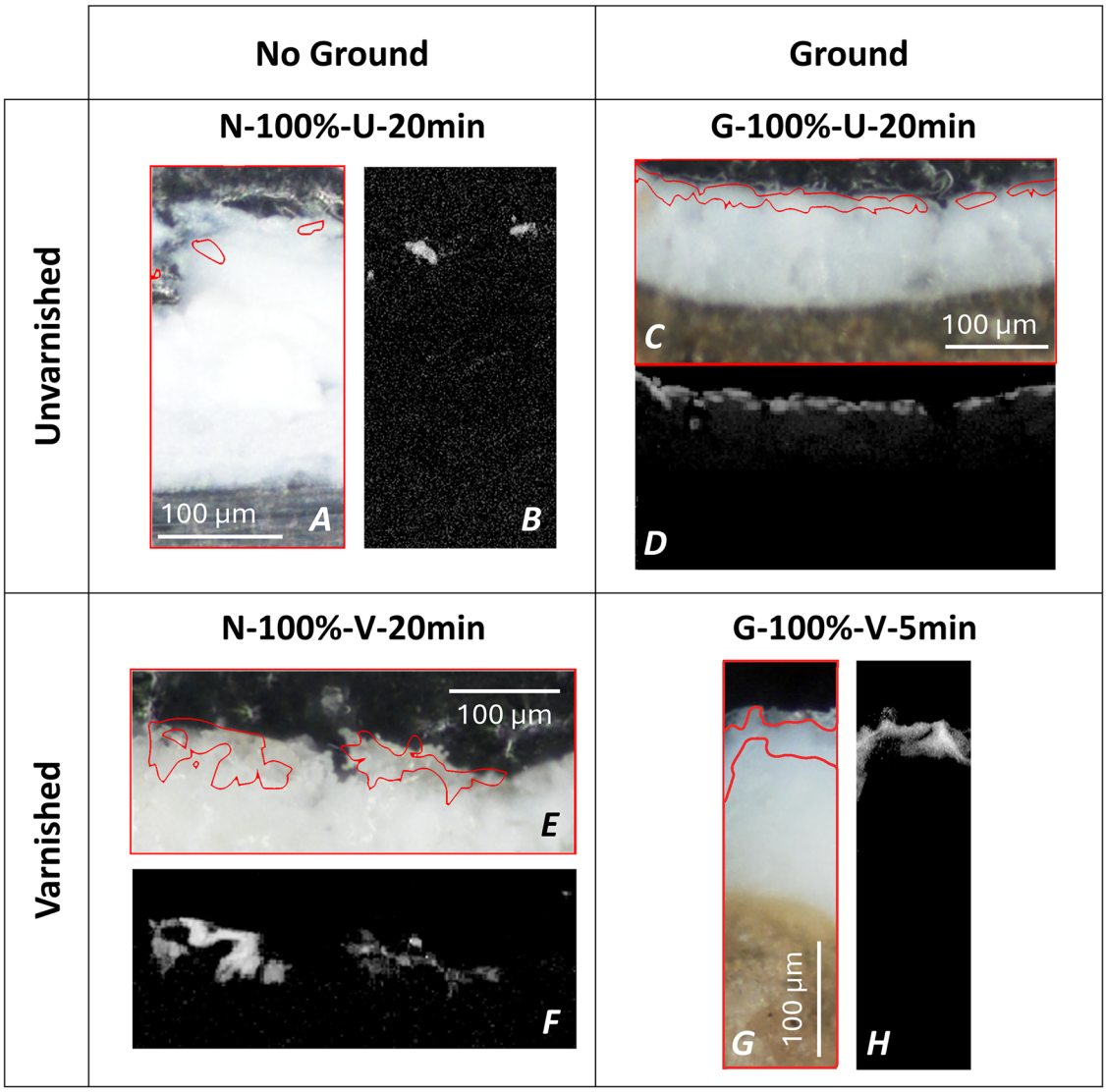

Fig. 8 | SR-µ-XRPD anglesite distribution maps of the paint mock-up samples. Samples containing 100% hydrocerussite exposure for 5 (**G**, **H**) or 20 min (**A**–**F**) to sulphuric acid; Samples without (left) and with (right) ground; Unvarnished (top) and varnished (bottom) samples. Brighter areas indicate a higher XRPD abundance value for anglesite.

encouraging outcome of this scientific research, there is currently no concern that the treatment will exacerbate any of the existing damage or that it will induce new issues within the affected area, as long as these areas will be treated with the utmost care.

In a more general sense, this research has demonstrated that the swift actions undertaken by the museum staff as part of the emergency response protocols appear to have been effective in protecting the integrity of the painting. Although small traces of the attack still remain, the dilution of the sulphuric acid with large volumes of demineralised water shortly after the attack, and the subsequent removal of the degraded varnish, protected the painting from further damage. However, the hydrophobic nature of the painting should not be disregarded as an important factor in the success of this particular case, especially when bearing in mind the lessons learned by other institutions regarding their experiences with water. It is therefore still recommended that future research be focused on a critical reassessment of the current emergency response protocols, and on whether they need to be adapted and implemented to ensure optimum protection for the collection's paintings that could be classified as more sensitive in similar emergency situations (i.e. panel, glue-paste lined and/or unvarnished paintings).

Data availability

All data needed to evaluate the conclusions in the paper are present in the paper and/or the supplementary information file. Additional data related to this paper may be requested from the authors.

Received: 5 June 2025; Accepted: 27 November 2025;
Published online: 02 March 2026

References

1. Metz, T. *Nachtwacht: Schrik Groter Dan Schade* (NRC Handelsblad, 1990). https://resolver.kb.nl/resolve?urn=KBNRC01:000029724:mpeg21:a0015.
2. van Duijn, E. & Filedt Kok, J. P. The restorations of Rembrandt's 'Night Watch'. In *The Art of Conservation* (eds, Martineau, J. & Bomford, D.) 268–303 (The Burlington Press, 2024).
3. Kuiper, L. & Hesterman, W. Restauratieverslag van Rembrandts Nachtwacht/Report on the Restoration of Rembrandt's Night Watch. *Bull. van. Het Rijksmus.* **24**, 14–51 (1976).
4. van Duijn, E. E. & Raven, L. Interview Martin Bijl (Rijksmuseum). DANS Data Station Social Sciences and Humanities, V2. (2019).
5. Mosk, J. Personal communication (oral history interview) with E. van Duijn, 4 November (2019).

6. de Keijzer, M. Personal communication (oral history interview) with E. van Duijn, 7 September (2021).
7. von Sonnenburg, H. & Heimberg, B. Säureanschlag auf drei Dürer-Werke in der Alten Pinakothek in München. Das Attentat und erste konservatorische Maßnahmen (Acid attack on three Dürer works in the Alte Pinakothek in Munich. The attack and initial conservation measures). *Restauro.* **96**, 13–21 (1990).
8. Burmester, A. & Koller, J. Säureanschlag auf drei Dürer-Werke in der Alten Pinakothek München. Schadenbeschreibung und Wege zur Konservierung aus naturwissenschaftlicher Sicht (Acid attack on three Dürer works in the Alte Pinakothek Munich. Damage description and approaches to conservation from a scientific perspective). *Restauro.* **96**, 89–95 (1990).
9. Burmester, A., Koller, J. & Kawinski, H. The Munich Dürer attack: the removal of sulphuric acid and acid compounds by use of a conditioned ion-exchange resin. In *Cleaning, Retouching and Coatings. Technology and Practice for Easel Paintings and Polychrome Sculpture* (eds, Mills, J. S. & Smith, P.) 177–183 (The International Institute for Conservation of Historic and Artistic Works, 1990).
10. Heimberg, B. The Munich Dürer attack: conservation and restoration of the damaged panels. In *Cleaning, Retouching and Coatings. Technology and Practice for Easel Paintings and Polychrome Sculpture* (eds, Mills, J. S., Smith, P.) 184–187 (The International Institute for Conservation of Historic and Artistic Works, 1990).
11. Heimberg, B. & Burmester, A. Die Retusche des Verlustes (Retouching the loss). In *Albrecht Dürer. Die Gemälde der Alten Pinakothek* (Albrecht Dürer. The Paintings of the Alte Pinakothek.) (eds, Goldberg, G., Heimberg, B. & Schawe, M.) 126–135 (Bayerische Staatsgemäldesammlungen München; 1998).
12. Peter, U. Zur Restaurierung des Rubensgemäldes ´Erzherzog Albrecht von Österreich' (On the restoration of the Rubens painting *Archduke Albert of Austria*). *Restauro.* **84**, 178–181 (1978).
13. von Sonnenburg, H. Rembrandts 'Segen Jakobs'. *Maltechnik Restauro.* **84**, 221–222 (1978).
14. Krämer, T., Ehrenforth, C. & Kammer, M. Zur Restaurierungsgeschichte der Werke Rembrandts, seiner Schüler und Werkstatt in der Kasseler Gemäldegalerie Alte Meister (On the restoration history of works by Rembrandt, his pupils, and his workshop in the Gemäldegalerie Alte Meister Kassel). *Z. für Kunsttechnol. Konservierung* **33**, 137–177 (2019).
15. Sokolova, I. Rembrandt's *Danaë* in the hermitage. A curriculum vitae. In *Danaja: sud'ba sedevra Rembrandta/Danaë: the fate of Rembrandt's masterpiece*, 124–141 (Sankt-Peterburg: Slavija, 1997).
16. Aleshina, T. Some problems concerning the restoration of Rembrandt's painting *Danaë*. In *Danaja: sud'ba sedevra Rembrandta/ Danaë: the fate of Rembrandt's masterpiece*, 142–146 (Sankt-Peterburg: Slavija, 1997).
17. Harrison L. *Chemical Attack: A Practical Survey. A Guide to Protocols and the Development of a Disaster Kit*. Unpublished postgraduate diploma dissertation (Courtauld Institute of Art, 1995).
18. Boitelle, R. Vandalisme en de eerste respons. Aanbevelingen naar aanleiding van de workshop aanvallen op schilderijen (Vandalism and the initial response. Recommendations following the workshop on attacks on paintings.). *Cr.* **2**, 14–20 (2002).
19. Blewett, M., Harrison, L. & Peggie, D. Incident preparedness at the National Gallery: developing a grab bag for rapid response to a corrosive attack. *Stud. Conserv.* **60**, 306–320 (2015).
20. Blewett, M., Harrison, L. & Peggie, D. Preparing for the worst: Re-developing and tailoring a rapid response 'Grab Bag' and procedure to the specific needs and limitations of the National Gallery, London. In *The AIC Paintings Specialty Group Postprints*, 25 (ed Buckley, B.) 15–24 (AIC; 2019).
21. de Meyer, S. et al. Imaging secondary reaction products at the surface of Vermeer's *Girl with the Pearl Earring* by means of macroscopic X-ray powder diffraction scanning. *Herit. Sci.* **7**, 1–11 (2019).
22. Alfeld, M. et al. A mobile instrument for in situ scanning macro-XRF investigation of historical paintings. *J. Anal. At. Spectrom.* **28**, 760–767 (2013).
23. Gabrieli, F. et al. Reflectance imaging spectroscopy (RIS) for Operation Night Watch: Challenges and achievements of imaging Rembrandt's Masterpiece in the glass chamber at the Rijksmuseum. *Sensors* **21**, 6855 (2021).
24. Legrand, S., Alfeld, M., Vanmeert, F., de Nolf, W. & Janssens, K. Macroscopic fourier transform infrared scanning in reflection mode (MA-rFTIR), a new tool for chemical imaging of cultural heritage artefacts in the mid-infrared range. *Analyst* **139**, 2489–2498 (2014).
25. Callewaert, T. et al. Multi-scale optical coherence tomography imaging and visualization of Vermeer's *Girl with a Pearl Earring*. *Opt. Express* **28**, 26239–26256 (2020).
26. Mosk, J. & de Keijzer, M. Rapportage over de meting van eventuele resten zwavelzuur op het oppervlak van de "Nachtwacht", na de aanslag op vrijdag 6 april 1990. (Report on the measurement of possible traces of sulfuric acid on the surface of The Night Watch after the attack on Friday, 6 April 1990.) Unpublished report (1990).
27. Gonzalez, V., van Loon, A., Price, S., Noble, P. & Keune, K. Synchrotron micro-XRD and XRD-CT reveal newly formed lead-sulfur compounds in Old Master paintings. *J. Anal. At. Spectrom.* **35**, 2267–2273 (2020).
28. Alfeld, M. & Janssens, K. Strategies for processing mega-pixel X-ray fluorescence hyperspectral data: a case study on a version of Caravaggio's painting *Supper at Emmaus*. *J. Anal. At. Spectrom.* **30**, 777–789 (2015).
29. Solé, V. A., Papillon, E., Cotte, M., Walter, P. & Susini, J. A multiplatform code for the analysis of energy-dispersive X-ray fluorescence spectra. *Spectrochim. Acta Part B* **62**, 63–68 (2007).
30. de Nolf, W., Vanmeert, F. & Janssens, K. XRDUA: crystalline phase distribution maps by two-dimensional scanning and tomographic (micro) X-ray powder diffraction. *J. Appl. Crystallogr.* **47**, 1107–1117 (2014).
31. van Loon, A., Keune, K. & Boon, J. J. Improving the surface quality of paint cross-sections for imaging analytical studies with specular reflection FTIR and Static-SIMS. In *Art'05—8th International Conference on "Non Destructive Investigations and Microanalysis for the Diagnostics and Conservation of the Cultural and Environmental Heritage"*. 15–19 (Lecce, Italy, Italian Society of NonDestructive Testing Monitoring Diagnostics, 2005).
32. Cotte, M. et al. The "Historical Materials BAG": a new facilitated access to synchrotron X-ray diffraction analyses for cultural heritage materials at the European Synchrotron Radiation Facility. *Molecules* **27**, 1–21 (2022). 1997.
33. Tauber, G. et al. Its use from a scientific and practical conservation perspective. *AIC Paint. Specialty Group Postprints* **31**, 45–50 (2018).
34. Baij, L. et al. Understanding and optimizing Evolon CR for varnish removal from oil paintings. *Herit. Sci.* **9**, 1–17 (2021).
35. De Mayerne, T. T., Versini, C. & Faidutti, M. *Le Manuscrit de Turquet de Mayerne* (Audin Imprimeurs; 1974).
36. Broers, F. T. H. et al. Correlated x-ray fluorescence and ptychographic nano-tomography on Rembrandt's *The Night Watch* reveals unknown lead "layer". *Sci. Adv.* **9**, 1–13 (2023).
37. Groen, K. Earth Matters. The origin of the material used for the preparation of *The Night Watch* and many other canvases in Rembrandt's workshop after 1640. *Art. Matters Neth. Tech. Stud. Art.* **3**, 138–154 (2005).
38. van de Laar, M. Personal communication with team *Operation Night Watch* (2019).
39. Gavrilenko, L. & Gerassimova, N. Paint layer cross-sections and colorimetric studies of Rembrandt's *Danaë*, damaged by sulphuric acid. In: *Danaja: sud'ba sedevra Rembrandta / Danaë: the fate of Rembrandt's masterpiece*, 147–153 (Sankt-Peterburg: Slavija, 1997).
40. Zoppi, A., Lofrumento, C., Mendes, N. F. C. & Castellucci, E. M. Metal oxalates in paints: a Raman investigation on the relative reactivities of

different pigments to oxalic acid solutions. *Anal. Bioanal. Chem.* **397**, 841–849 (2010).
41. Cariati, F., Rampazzi, L., Toniolo, L. & Pozzi, A. Calcium oxalate films on stone surfaces: experimental assessment of the chemical formation. *Stud. Conserv.* **45**, 180–188 (2000).
42. Keune, K., van Loon, A. & Boon, J. J. SEM backscattered-electron images of paint cross sections as information source for the presence of the lead white pigment and lead-related degradation and migration phenomena in oil paintings. *Microsc. Microanal.* **17**, 696–701 (2011).
43. van Loon, A. et al. Beauty is skin deep: the skin tones of Vermeer's *Girl with a Pearl Earring*. *Herit. Sci.* **7**, 1–20 (2019).
44. Price, S. W. T. et al. Unravelling the spatial dependency of the complex solid-state chemistry of Pb in a paint micro-sample from Rembrandt's *Homer* using XRD-CT. *Chem. Commun.* **55**, 1931–1934 (2019).
45. van Loon, A. et al. *Metal Soaps in Art*, 283–296 (Springer, 2019).
46. Vanmeert, F. et al. Transmission and reflection mode macroscopic X-ray powder diffraction imaging for the noninvasive visualization of paint degradation in still life paintings by Jan Davidsz. *De. Heem. Anal. Chem.* **91**, 7153–7161 (2019).
47. van Loon, A. et al. Artificial orpiment, a new pigment in Rembrandt's palette. *Herit. Sci.* **5**, 26 (2017).
48. van Loon A., Noble P. & Boon J. J. White hazes and surface crusts in Rembrandt's *Homer* and related paintings. In *ICOM Committee for Conservation 16th Triennial Meeting, Lisbon* (ed. Bridgland, J.) 1–10 (ICOM, 2011).
49. van Loon A., Noble P. & Boon J. J. The formation of complex crusts in oil paints containing lead white and smalt: dissolution, depletion, diffusion, deposition. In: *Historical Technology, Materials and Conservation: SEM and Microanalysis* (eds, Meeks, N., Cartwright, A. & Mongiatti, A.) 205–207 (Archetype Publications, 2012).
50. van der Snickt, G. et al. Characterization of a degraded cadmium yellow (CdS) pigment in an oil painting by means of synchrotron radiation based X-ray techniques. *Anal. Chem.* **81**, 2600–2610 (2009).

Acknowledgements

The authors are indebted to the team members of *Operation Night Watch*, in particular Cindy Doff, Robert Erdmann, Nouchka de Keyser, Petria Noble, Susan Smelt, Ige Verslype, Lisette Vos and Carola van Wijk, for their assistance during the research activities and their participation in valuable discussions concerning this topic. The main partner of *Operation Night Watch* is AkzoNobel. *Operation Night Watch* is made possible by The Bennink Foundation, C.L. de Carvalho-Heineken, PACCAR Foundation, Piet van der Slikke & Sandra Swelheim, American Express Foundation, Familie De Rooij, Het AutoBinck Fonds, TBRM Engineering Solutions, Dina & Kjell Johnsen, Familie D. Ermia, Familie M. van Poecke, Bruker Nano Analytics, Henry M. Holterman Fonds, Irma Theodora Fonds, Luca Fonds, Piek-den Hartog Fonds, Stichting Zabawas, Cevat Fonds, Johanna Kast-Michel Fonds, Marjorie & Jeffrey A. Rosen, Stichting Thurkowfonds, Familie Van Ogtrop Fonds, FedEx Express, Airbnb, NICAS, the Night Watch Fund, the City of Amsterdam and the Amsterdam Museum. In addition, gratitude is extended to thank Martin Bijl, Michel van de Laar, Matthijs de Keijzer and Jaap Mosk for their readiness to disseminate any information regarding the events on the day of the attack, and to the guards, Paul Donker and Frank Wessels (then called Frank Wildschut), who acted with immediate effect and prevented more substantial harm to the painting. Additionally, the authors would like thank the staff at PETRA-III Beamline P06 during the micro-XRPD characterisation experiments of the original and mock-up paint samples, in particular Jan Garrevoet, Ken Vidar Falch and Gerald Falkenberg. The European Synchrotron Radiation Facility is acknowledged for the provision of synchrotron radiation facilities, and assistance in using beamline ID13 (proposal HG-213), pilot of a BAG project supported by the European Union's Horizon 2020 research and innovation program under grant agreement No 870313, Streamline. The authors would like to express their gratitude to Manfred Burghammer, Marine Cotte, Ida Fazlic and Clement Hole for their contributions. The authors acknowledge financial support from the FWO Brussels, through a grant from the FWO project: a combined IR, NIR and MA-XRF material inspection method with FWO ID G056619 N and from Interreg Vlaanderen-Nederland (Smart*Light 2.0 project). Finally, we acknowledge Thorlabs, Inc. for providing the OCT Ganymede 930 nm system for Operation Night Watch.

Author contributions

L.R. performed the stereomicroscopy and varnish removal tests, took and embedded the paint samples, performed the light microscopy, and assisted in the acquisition of the OCT, SEM-EDX, μ-ATR-FTIR, MA-XRF, MA-XRPD data. E.A.C. and K.J. designed the reconstructions. A.G., E.A.C. and S.d.M. analysed the reconstructions. A.v.L. acquired and processed the MA-XRF, SEM-EDX and μ-ATR-FTIR data. A.v.L. and L.R. interpreted the SEM-EDX and μ-ATR-FTIR data. V.G. acquired and processed the MA-XRF data, and assisted in the acquisition of the MA-XRPD data. A.G., F.V. and S.d.M. acquired and processed the MA-XRPD data. S.d.M., V.G., F.V. and A.G. acquired and processed the SR-μ-XRPD data of sample SK-C-5_024a; A.G. and E.A.C. acquired and processed the SR-μ-XRPD data of sample SK-C-5_035 and SK-C-036. L.R., A.G., A.v.L., E.A.C., K.J., K.K. interpreted the MA-XRF, MA-XRPD, and SR-μ-XRPD data. M.A. acquired and processed the OCT data. M.A. and L.R. interpreted the OCT data. E.v.D. and L.R. conducted the conservation history research. L.R. and A.G. wrote the main body of the text. L.R., A.G., A.v.L., E.v.D., E.A.C., S.d.M., K.J. and K.K. edited the text. K.K. and K.J. supervised the project. All authors read and approved the final manuscript.

Competing interests

The authors declare no competing interests.

Additional information

Supplementary information The online version contains supplementary material available at https://doi.org/10.1038/s40494-025-02233-5.

Correspondence and requests for materials should be addressed to Laura Raven.